Design of dispersion flattened photonic crystal fiber with a large core and a concentric missing ring

Design of dispersion flattened photonic crystal fiber with a large core and a concentric missing ring

Koichi Iiyama, Zennosuke Yamashita, and Saburo Takamiya
Division of Electrical Engineering and Computer Science
Graduate School of Natural Science and Technology, Kanazawa University
Kakuma-machi, Kanazawa, Ishikawa, 920-1192 Japan
E-mail: iiyama@ee.t.kanazawa-u.ac.jp

***Abstract*—Novel structure of an index-guiding photonic crystal fiber (PCF) is proposed for flattened dispersion characteristics. As compared with the conventional PCFs, the proposed PCF has a following feature in its structure; the first ring area contains no air holes, and the third ring area also contains no air holes. Then the proposed PCF has a large core and a concentric missing ring. The chromatic dispersion was numerically simulated by the semi-vector finite difference method. The chromatic dispersion becomes almost flat in 1300 ~ 1650 nm wavelength range when the air hole diameter is about 0.35 times the air hole spacing. Especially the chromatic dispersion is -1 ~ 0 (ps/nm/km) in the above wavelength range when the air hole spacing is 1.25 μm and the air hole diameter is 0.43 μm.**

I. INTRODUCTION

In recent years, photonic crystal fibers (PCFs), also called holey fibers (HFs), are actively studied [1-3]. The PCFs consist of a central defect region surrounded by periodic air holes along its length. The chromatic dispersion of the PCFs can be controlled by changing the air hole spacing Λ and the air hole diameter *d*. Zero dispersion in visible and near-infrared wavelengths is achieved by increasing the ratio of the air hole diameter to the air hole spacing d / Λ [4-5]. Nearly zero dispersion-flattened PCFs around 1550 nm wavelength region are proposed by decreasing the d / Λ [6-7], and by gradually increasing the air hole diameter in the lateral direction [8].

In this paper, we proposed a novel structure of a dispersion-flattened PCF in long wavelength region. The features of the PCF are that the center core is larger than that of conventional PCFs and the concentric core is introduced. The effective index, the mode profile, the chromatic dispersion, and the effective mode area are numerically simulated by the semi-vectorial finite different method.

II. PROPOSED STRUCTURE

Figure 1 shows the structure of the proposed PCF. The conventional PCF has only one missing air hole in the center of the PCF, which acts as a core of the PCF, and six air holes are arranged in the first ring area. Whereas, in the proposed PCF, the first ring area contains no air holes. As a result, the core is composed of seven missing air holes, and the core diameter is almost twice as large as that of the conventional PCF with the same air holes spacing. The third ring area also contains no air holes, which forms a concentric missing ring. The second ring area and the outer region contain air holes with triangular arrangement, like conventional PCFs. The light is well confined within the center core despite of existence of the concentric missing ring because of the large core diameter. The design parameters are only the air hole spacing and the air hole diameter.

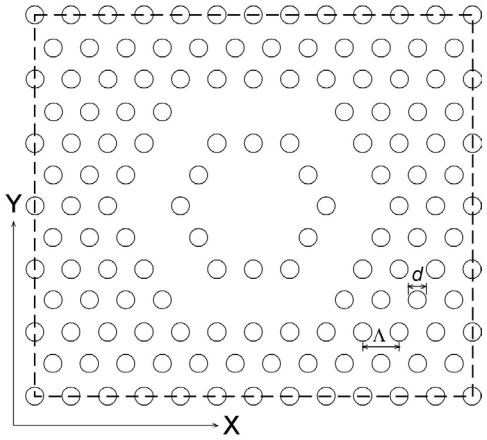

Fig. 1. The structure of the proposed PCF.

In the proposed PCF, the chromatic dispersion is controlled by interaction between the propagation modes of the center core and the concentric missing ring, which is called super mode [9]. The chromatic dispersion is numerically simulated by the semi-vectorial finite difference method for TE mode (X-polarization). The simulation area is shown as dashed lines in Fig. 1, and the Neumann boundary condition is used for the simulation boundaries. The mesh size for both the X and Y direction is (6 x Λ) / 200 in our simulation, which gives about 30 ~ 40 nm mesh size. The material of the PCF is pure silica, and the material dispersion by Sellmeier's formula is directly included in the simulation. The effective index n_{eff} is numerically calculated and the chromatic dispersion D is obtained by;

$$D = -\frac{\lambda}{c}\frac{d^2 n_{eff}}{d\lambda^2}$$

where c and λ are the velocity of light in vacuum and the wavelength, respectively.

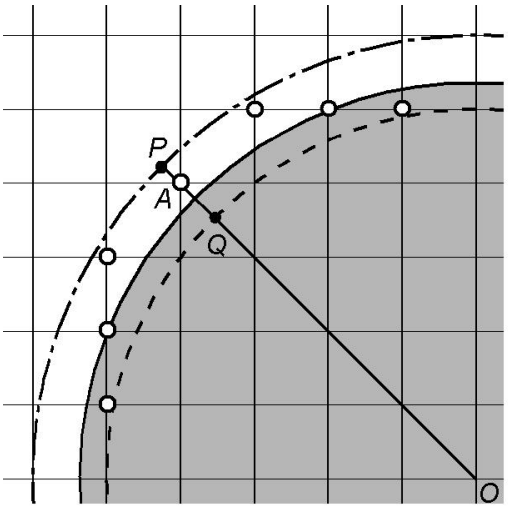

Fig.2. Index averaging.

To improve the simulation accuracy, the refractive indices around the air hole interfaces are approximated by the averaged value of the two mesh points across the interface [10]. Figure 2 shows the structure and the simulation mesh around the air hole interface. The dark area is the air hole, and the thin orthogonal lines are the simulation mesh. The point O is the center of the air hole, and the mesh size for both the X and Y direction is δ. The dot line shows the largest concentric circle inside the air hole whose radius is given by integer multiple of the mesh size δ, and the dash-dot line shows the smallest concentric circle outside the air hole whose radius is given by integer multiple of the mesh size δ.

The refractive index of the mesh points inside the dot line is 1.0, and the refractive index of the mesh points outside the dash-dot line is given by the refractive index of pure silica. The index averaging is applied to the mesh points indicated by open circles. For example, the refractive index of the mesh point A, n_A, is given by linear interpolation between the points P and Q, and is calculated as;

$$n_A = n_P \frac{\overline{OA} - \overline{OQ}}{\delta} + n_Q \frac{\overline{OP} - \overline{OA}}{\delta}$$

where $\overline{OA}$, $\overline{OQ}$ and $\overline{OP}$ are the length between the points O an A, the length between the points O and Q, and the length between the points O and P, respectively, and n_P and n_Q are the refractive indices of the points P and Q, respectively.

III. Simulation Results

A. Mode field and effective index

At first, we show the results on the mode field. Figures 3 and 4 show the simulated mode field of the PCF with Λ = 2.0 μm and d = 0.5 μm at 600 nm and 1550 nm wavelengths, respectively. In both figures, (a) shows the mode field of the fundamental mode, and (b) shows the mode field of the 1st higher order mode. The mode field of the fundamental mode is single-peak shape and is well confined within the center core region, and the mode field

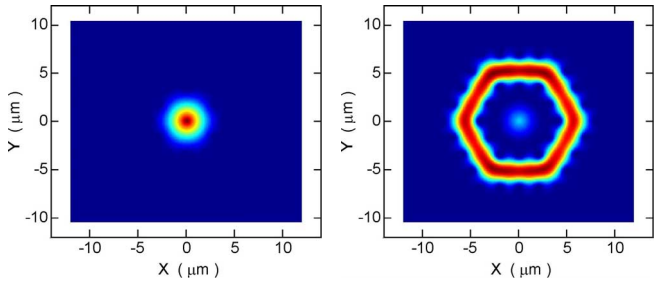

Fig. 3. Simulated mode field of the PCF with Λ = 2.0 μm and d = 0.5 μm at 600 nm wavelength.

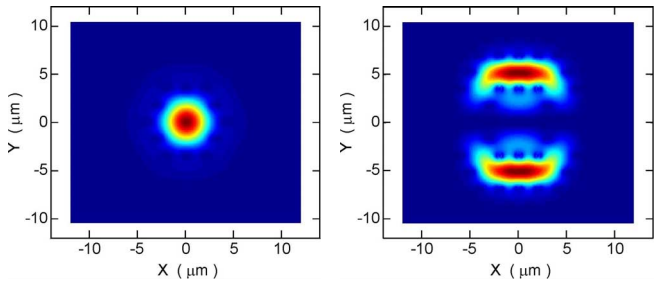

Fig. 4. Simulated mode field of the PCF with Λ = 2.0 μm and d = 0.5 μm at 1550 nm wavelength.

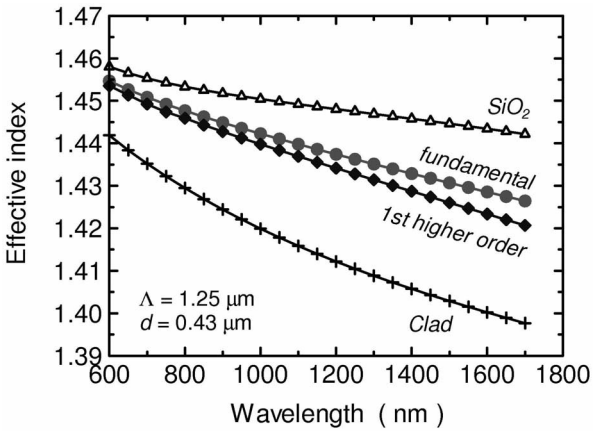

Fig. 5. Simulated effective index of the PCF with Λ = 1.25 μm and d = 0.43 μm.

of the 1st higher order mode is distributed in the concentric missing ring. No mode field with multiple peaks within the center core is obtained in the calculated wavelength range (Λ > 600 nm). This means the PCF is endlessly single-moded.

Figure 5 shows the effective indices of the fundamental and the 1st higher order modes of the PCF with Λ = 1.25 μm and d = 0.43 μm. In the figure, the curve labeled "SiO_2" is the refractive index of pure silica calculated from the Sellmeier's formula, and the curve labeled "Clad" is the effective clad index given by the effective index of the space-filling mode in the clad region. The effective index difference between the fundamental and the 1st higher order modes increases with the wavelength, and the difference is 4.92 x 10^{-3} at 1550 nm wavelength. If the effective index difference between the fundamental and the 1st higher order modes is small, coupling of the propagating light between

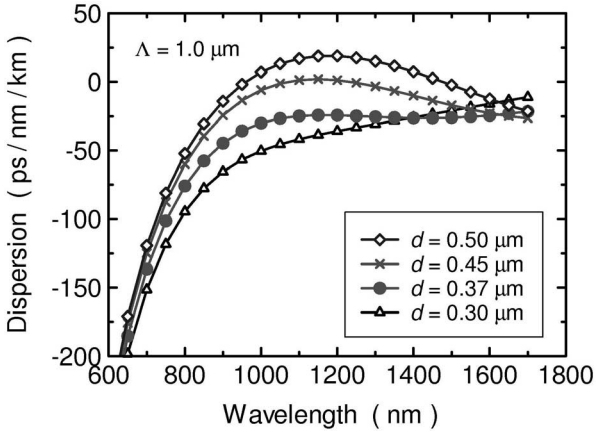

(a) Air hole spacing Λ = 1.0 μm

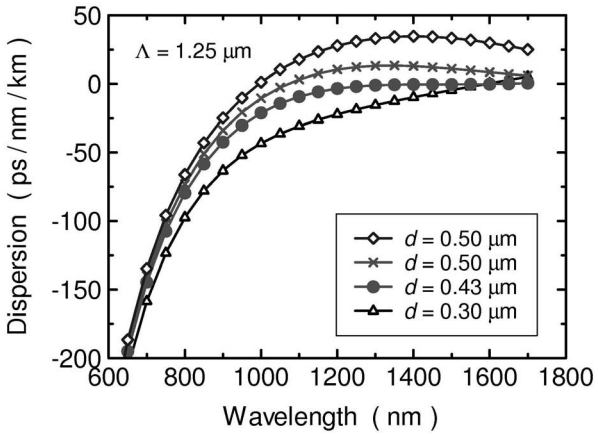

(a) Air hole spacing Λ = 1.25 μm

Fig. 6. Simulated chromatic dispersion of the proposed PCF for different values of the air hole diameter *d*.

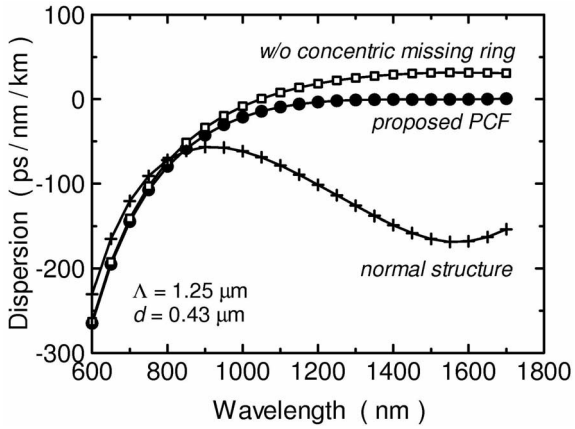

Fig. 7. Simulated chromatic dispersion of the proposed PCF with Λ = 1.25 μm and d = 0.43 μm

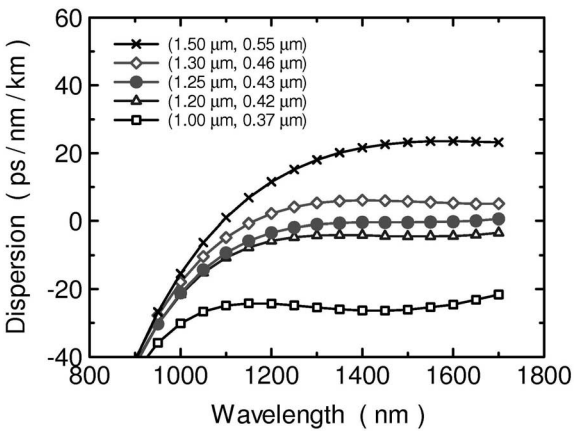

Fig. 8. Simulated chromatic dispersion of the proposed PCF for different values of the air hole spacing and the air hole diameter pairs (Λ, *d*). The ratio *d* / Λ is about 0.35 for all the structures.

the center core and the concentric missing ring may occur because the structure is like a directional coupler. In birefringent optical fibers, the birefringence of the order of 10^{-3} is enough to prevent polarization coupling between the orthogonal polarizations. Deducing from polarization stability in birefringent optical fibers, we think that the effective index difference of the order of 10^{-3} between the fundamental and the 1st higher order modes is enough so that the light propagates in the large center core region without being coupled to the concentric missing ring when the light is launched into the large center core region.

B. Chromatic Dispersion

Figure 6 shows the simulated chromatic dispersion of the proposed PCF for different values of the air hole diameter *d*. The air hole spacing is (a) Λ = 1.0 μm and (b) Λ = 1.25 μm. The chromatic dispersion is almost flattened in 1300 ~ 1650 nm wavelength range when *d* = 0.37 μm for Λ = 1.0 μm and when *d* = 0.43 μm for Λ = 1.25 μm. When the *d* is smaller than the above value, the chromatic dispersion increases against the wavelength. When the *d* is larger than the above value, the chromatic dispersion increases until certain wavelength (1150 nm for Λ = 1.0 μm and 1350 nm for Λ = 1.25 μm), and then decreases against the wavelength.

Figure 7 shows the simulated chromatic dispersion of the proposed PCF with Λ = 1.25 μm and *d* = 0.43 μm. The closed circles are the chromatic dispersion with the proposed structure, the open squares are the chromatic dispersion with large center core region and without the concentric missing ring, and the crosses are the chromatic dispersion of a PCF with normal structure (single missing ring in the center core and no concentric missing ring). The structure of the large center core makes the chromatic dispersion property flat in long wavelength region, and the value of the chromatic dispersion in long wavelength region decreases by introducing the concentric missing ring.

Figure 8 shows the simulated chromatic dispersion for different values of the air hole spacing and the air hole diameter pair, (Λ, *d*). The values of *d* / Λ are about 0.35 for all structures. Negative flattened dispersion is achieved when Λ < 1.25 μm, and positive flattened dispersion is achieved when Λ > 1.25 μm. Especially the chromatic dispersion is nearly zero (-1 ~ 0 ps/nm/km) in 1300 ~ 1650 nm wavelength range when Λ = 1.25

TABLE 1
SUMMARY OF THE SIMULATED CHROMATIC DISPERSION IN 1300 ~ 1650 NM WAVELENGTH RANGE.

Λ	d	d/Λ	Disersion
1.00 μm	0.38 μm	0.380	-24.496 ± 1.216 ps/nm/km
1.20 μm	0.42 μm	0.350	-4.239 ± 0.219 ps/nm/km
1.25 μm	0.43 μm	0.344	-0.451 ± 0.517 ps/nm/km
1.26 μm	0.44 μm	0.349	1.316 ± 0.252 ps/nm/km
1.30 μm	0.46 μm	0.354	5.572 ± 0.543 ps/nm/km
1.50 μm	0.52 μm	0.347	16.722 ± 2.753 ps/nm/km
1.50 μm	0.55 μm	0.367	20.781 ± 2.770 ps/nm/km

μm and d = 0.43 μm.

The obtained flattened chromatic dispersion is summarized in Table 1, where value of the d is the value when the most flattened chromatic dispersion is achieved for a given Λ. The relative air hole diameter d/Λ is almost 0.35 for all the structure. The flatness is less than ± 1 ps/nm/km when Λ is the range 1.2 μm < Λ < 1.3 μm, and the flatness is degraded with increasing and decreasing the Λ.

C. Effective Mode Area

The simulated effective mode area of the proposed PCF against the wavelength is shown in Fig. 9. The effective mode area A_{eff} is calculated as;

$$A_{eff} = \frac{\left[\iint |E|^2 \, dxdy\right]^2}{\iint |E|^4 \, dxdy}.$$

The air hole spacing and the air hole diameter are Λ = 1.25 μm and d = 0.43 μm, respectively. The effective mode area increases in longer wavelength by introducing the concentric core, and the effective mode area is 17 μm^2 at 1550 nm wavelength. Although the effective mode area is smaller than that of conventional dispersion shifted fibers (about 50 μm^2), it is larger than that of the dispersion-flattened PCFs proposed by other groups (10 ~ 13 μm^2).

IV. CONCLUSION

We have proposed a novel structure of dispersion-flattened PCF. The features of the PCF are that the center core is larger than that of conventional PCFs and the concentric missing ring is introduced. The structure of the large center core makes the chromatic dispersion property flat in long wavelength region, and the value of the chromatic dispersion in long wavelength region decreases by introducing the concentric missing ring. Negative, positive, and nearly zero flattened dispersions are achieved by changing the air hole spacing Λ while keeping the relative air hole diameter d/Λ be about 0.35.

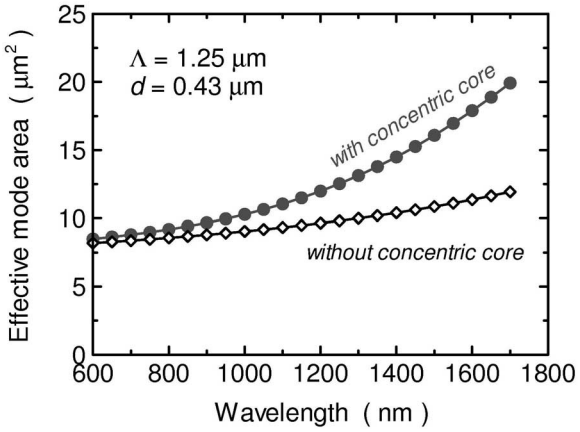

Fig. 9. Simulated mode area of the PCF with Λ = 1.25 μm and d = 0.43 μm

REFERENCES

[1] Knight, T.A. Birks, P.St.J. Russel, and D.M. Atkin, "All-silica single-mode optical fiber with photonic crystal cladding", *Opt. Lett*., **21**, pp. 1547-1549 (1996)

[2] J. Broeng, D. Mogilevstev, S.E. Barkou, and A. Bjarklev, "Photonic crystal fibers: a new class of optical waveguides", *Optical Fiber Technology*, **5**, pp. 305-330 (1999).

[3] T.A. Briks, J.C.Knight, B.J. Mangan, and P.St.J. Russel, "Photonic crystal fibers: an endless variety", *IEICE Trans. Electron.*, **E84-C**, pp. 585-592 (2001).

[4] M.J. Gander, *et. al.*, "Experimental measurement of group velocity dispersion in photonic crystal fiber", *Electron. Lett.*, **35**, pp. 63-64 (1999).

[5] J.C. Knight, *et. al.*, "Anomalous dispersion in photonic crystal fiber", *IEEE Photon. Technol. Lett.*, **12**, pp. 807-809 (2000).

[6] A. Ferrando, E. Silvestre, P. Andres, J.J. Miret, and M.V. Andres, "Designing the properties of dispersion-flattened photonic crystal fibers", *Opt. Express*, **9**, pp. 687-697 (2001).

[7] L.P. Shen, W.P Huang, and S.S. Jian, "Design of photonic crystal fibers for dispersion-related applications", *J. Lightwave Technol*., **21** pp. 1644-1651 (2003).

[8] K. Saito, M. Koshiba, T. Hasegawa, and E. Sasaoka, "Chromatic dispersion control in photonic crystal fibers: application to ultra-flattened dispersion", *Opt. Express*, **11**, pp. 843-852 (2003).

[9] K. Thyagarajan, R.K. Varshney, P. Palai, A.K. Ghatak, and I.C. Goyal, "A novel design of a dispersion compensating fiber", *IEEE Photon. Technol. Lett.*, **8**, pp. 1510-1512 (1996).

[10] Z. Zhu and T.G. Brown, "Full-vectorial finite-difference analysis of microstructured optical fibers", *Opt. Express*, **10**, pp. 853-864 (2002).